Dengue virus M and E proteins belonging to genotype II (Cosmopolitan) of serotype 2 are influenced by the nature of M residue 36

Jason Decotter, Philippe Desprès, Gilles Gadea

JOURNAL OF GENERAL VIROLOGY

RESEARCH ARTICLE

Decotter *et al.*, *Journal of General Virology* 2023;104:001872

DOI 10.1099/jgv.0.001872

MICROBIOLOGY SOCIETY

OPEN ACCESS

Dengue virus M and E proteins belonging to genotype II (Cosmopolitan) of serotype 2 are influenced by the nature of M residue 36

Jason Decotter, Philippe Desprès* and Gilles Gadea†

Abstract

Mosquito-borne dengue disease is caused by the dengue virus serotype-1 to serotype-4. The contemporary dengue outbreaks in the southwestern Indian ocean coincided with the widespread of dengue virus serotype 2 genotype II (Cosmopolitan), including epidemic viral strains DES-14 and RUN-18 isolated in Dar es Salaam (Tanzania) in 2014 and La Reunion Island (France) in 2018, respectively. Heterodimeric interaction between prM (intracellular precursor of surface structural M protein) and envelope E proteins is required during the initial stage of dengue virus assembly. Amino acid 127 of DES-14 prM protein (equivalent to M36) has been identified as an infrequent valine whereas RUN-18 has a common isoleucine. In the present study, we examined the effect of M-I36V mutation on the expression of a recombinant RUN-18 E protein co-expressed with prM in human epithelial A549 cells. The M ectodomain of dengue virus serotype 2 embeds a pro-apoptotic peptide referred as D_2AMP. The impact of M-I36V mutation on the death-promoting capability of D_2AMP was assessed in A549 cells. We showed that valine at position M36 affects expression of recombinant RUN-18 E protein and potentiates apoptosis-inducing activity of D_2AMP. We propose that the nature of M residue 36 influences the virological characteristics of dengue 2 M and E proteins belonging to genotype II that contributes to global dengue burden.

INTRODUCTION

Dengue is a mosquito-borne viral disease of major public health problem worldwide, primarily in tropical and subtropical regions [1, 2]. Dengue disease is caused by dengue virus (DENV), a mosquito-borne RNA virus belonging to the *Flavivirus* genus (*Flaviviridae* family) which includes other medically-important arthropod-borne viruses such as Japanese encephalitis virus (JEV), tick-borne encephalitis virus (TBEV), West Nile virus (WNV), yellow fever virus (YFV), and Zika virus (ZIKV). DENV is categorized into four serotypes DENV-1 to DENV-4. Infection can occur with one or more of the four serotypes. Infection with one serotype provides lifelong homotypic immunity to that particular serotype but does not confer long-term protection against infection by other serotypes. DENV infection can result in a wide range of clinical manifestations, from flu-like disease (dengue fever) to severe illness (severe dengue), a potentially lethal disease [3, 4].

DENV contains a positive-sense single-stranded RNA encoding a single large polyprotein precursor that is co- and post-translationally processed by host and viral protease into three structural proteins which are the capsid protein (C), the precursor membrane protein (prM) and the envelope protein (E), followed by seven nonstructural proteins [5]. DENV E glycoprotein (495 amino-acid residues) is involved in virus attachment to host-cell, in internalization of virus particles, and then in the fusion between viral and cellular membranes releasing genomic RNA into the cytosol. The ectodomain of DENV E protein is organized into three structurally envelope domains EDI, EDII, and EDIII [6]. The EDII contains the viral fusion peptide (residues E98-112)

Received 11 March 2023; Accepted 24 June 2023; Published 12 July 2023

Author affiliations: [1]Processus Infectieux en Milieu Insulaire Tropical (PIMIT), Université de La Réunion, INSERM U1187, CNRS 9192, IRD 249, Plateforme Technologique CYROI, 97490 Sainte-Clotilde, La Réunion, France.

***Correspondence:** Philippe Desprès, philippe.despres@univ-reunion.fr

Keywords: arbovirus; flavivirus; dengue 2 virus; genotype II; M protein; E protein; apoptotic viral peptide.

Abbreviations: ApoptoM, dengue M apoptotic oligopeptide; CLS, crown-like structure; CNX, calnexin protein; ER, endoplasmic reticulum; FACS, fluorescence-activated cell sorting; GAPDH, glyceraldehyde-3-phosphate dehydrogenase; GFP, green fluorescent protein; IF, immunofluorescence; LDH, lactate dehydrogenase; mAb, monoclonal antibody; MFI, mean fluorescence intensity; MTT, 3-[4,5-dimethylthiazol-2yl]-2,5-diphenyltetrazolium bromide; SP, signal peptide; SWIO, South West Indian Ocean; TMD, transmembrane domain.

†Present address: MetaSarc team Inserm U1194, Institut de Recherche en Cancérologie de Montpellier (IRCM), F-34298 Montpellier, France.

Three supplementary figures and two supplementary tables are available with the online version of this article.

whereas EDIII may play a key role in virus binding to the host-cell receptor [7, 8]. DENV prM glycoprotein (166 amino-acid residues) consists of 'pr' peptide (residues prM1-91) followed by the surface structural M protein (residues prM92-166) [9]. The initial step of virus assembly involves heterodimeric interactions between prM and E proteins, prM playing the role of chaperone for E to prevent a premature fusion of immature virus particles during their transport through the secretory pathway [10, 11]. The heterodimeric interactions between prM and E proteins are important for the proper folding of E [12, 13]. The processing of prM occurs in the trans-Golgi apparatus by cellular furin/furin-like protease family that cleaves the 'pr' peptide from the surface membrane M protein [14]. In the topology of prM-E heterodimer, the M protein appears to be adjacent to EDII [11, 15]. The M protein consists of an N-terminal ectodomain (referred hereafter as ectoM) which is formed of a flexible hydrophobic loop followed by an amphipathic peri-membrane α-helix and ended by a C-terminal transmembrane region [11]. It has been reported that DENV-2 ectoM conjugated to a reporter protein such as GFP can trigger apoptosis [16]. The apoptosis-inducing activity of ectoM requires caspase-3 activation and its transport in the secretory pathway is a pre-requisite for initiation of apoptosis [16, 17]. The death-promoting capability of DENV-2 M protein has been restricted to an oligopeptide representing the C-terminal amino-acids of M ectodomain [16]. Amino acid 36 of the M protein (equivalent to prM127) has been identified as playing an important role in several aspects of virus replication cycle [18–20]. Indeed, M36 mutations may have an effect on virus assembly and/or egress and thus, modulate the pathogenicity of flaviviruses [18, 19].

Dengue outbreaks in the tropics are mostly associated with DENV-2 and increasing geographic distribution of genotype II (or Cosmopolitan genotype) contributes to the global dengue burden [21]. Genotype II of DENV-2 is circulating in Africa, Asia, the Middle East, the Pacific Islands and now South America [22]. Over the last decade, southwestern Indian ocean countries have been facing to the emergence of DENV-2 genotype II [23–25]. In 2018–19, Reunion Island experienced a dengue epidemic with nearly 25000 cases reported out of a population of 875000 inhabitants [26–28]. DENV-2 strains isolated from dengue patients in 2018 were sequenced and phylogenetic analysis reported that all DENV-2 clinical isolates belong to the genotype II, Cosmopolitan 1 (C1-B) lineage, including the prototypical RUJul strain (RUN-18, Genbank accession number MN272404.1) [23, 24]. In the southwestern Indian ocean region, other epidemic DENV-2 strains of Cosmopolitan lineage were also sequenced. The dengue outbreak that occurred in Dar es Salaam (Tanzania) in 2014 was associated with DENV-2 genotype II, Cosmopolitan 2 lineage. During the epidemic, the DENV-2 strain D2_K2_RIJ_059/Dar es Salaam 2014 (DES-14, GenBank accession number MG189962.1) was isolated from a patient with dengue fever [25]. Comparative sequence analysis between the M proteins of DENV-2 strains RUN-18 and DES-14 identified an infrequent valine at residue 36 of DES-14 whereas RUN-18 has a common isoleucine. It is suspected that M residue 36 might have an impact on the biological properties of DENV-2 envelope proteins. In the present study, the effects of Ile-to-Val mutation at position M36 on the expression of the E protein and death-promoting capability of M peptide were assessed on recombinant viral proteins derived from DENV-2 strain RUN-18.

METHODS

Cell culture, antibodies and reagents

For cell culture, human lung carcinoma epithelial A549 cells (ATCC, CCL-185) were cultured in Dulbecco's Modified Eagle's Medium (DMEM) supplemented with 10% heat-inactivated fetal bovine serum (FBS) (Dutscher, Brumath, France), 2 mmol.L^{-1} of L-Glutamine, 1 mmol.L^{-1} of sodium pyruvate, 100 U.mL^{-1} of penicillin, 0.1 mg.mL^{-1} of streptomycin and 0.5 µg.mL^{-1} of fungizone (Amphotericin B) (PAN Biotech, Aidenbach, Germany) at 37 °C under 5% CO_2 atmosphere. The mouse anti-pan flavivirus envelope E glycoprotein domain II (EDII) monoclonal antibody (mAb) 4G2, purchased from RD Biotech (Besançon, France), and the mouse anti-DENV envelope E glycoprotein domain III (EDIII) mAb 4E11, a kind gift of Pasteur Institute (Paris, France), were used for immunodetection of the viral envelope E protein. Mouse anti-6x(His) mAb was purchased from Abcam (Cambridge, UK), to detect NS1 protein expression. Rabbit anti-calnexin antibody was purchased from Santa-Cruz Biotechnology (Clinisciences, Nanterre, France) and rabbit anti-β actin antibody from ABclonal (Massachusetts, USA), to detect the ubiquitously and constitutively expressed Calnexin and β actin proteins respectively. Donkey anti-mouse Alexa Fluor 488 and donkey anti-rabbit Alexa Fluor 594 secondary antibodies were purchased from Invitrogen (Carlsbad, CA, USA). Goat anti-mouse and goat anti-rabbit immunoglobulin-horseradish peroxidase (HRP) conjugated antibodies were purchased from Abcam (Cambridge, UK). Blue-fluorescent DNA stain 4',6-diamidino-2-phenylindole (DAPI) was purchased from Euromedex (Souffelweyersheim, France). Lipofectamine 3000 (Thermo Fisher Scientific, Les Ulis, France) was used for transfection, according to the manufacturer's instructions.

Vector plasmids expressing recombinant dengue proteins

A mammalian codon-optimized synthetic gene coding for the RUN-18 prM protein followed by the E protein (Genbank accession number MN272404.1) and preceded by the RUN-18 prM signal peptide was chemically synthesized and then inserted into *Nhe* I and *Not* I restriction sites of vector plasmid pcDNA-3.1 by Genecust (Boynes, France). Site-directed mutagenesis was performed on resulting plasmid pcDNA3/RUN-18 prME to generate mutants bearing M-(E33A, W35A, R38A), M-(I36A) or M-(I36V) mutation by Genecust (Boynes, France). A mammalian codon-optimized synthetic gene coding for the reporter gene GFP followed by the RUN-18 ectoM (ectoM^{RUN-18}, RUN-18 residues M1/41) or D_2AMP^{RUN-18} sequence (RUN-18 M31/41 residues)

(Genbank accession number MN272404.1) and preceded by the RUN-18 prM signal peptide was inserted into *Nhe* I and *Not* I restriction sites of vector plasmid pcDNA-3.1 by Genecust (Boynes, France). A short Gly-Ser spacer was inserted between sGFP and RUN-18 M sequences. Site-directed mutagenesis was performed on resulting plasmids pcDNA3/sGFP- ectoM^{RUN-18} and pcDNA3/sGFP-D$_2$AMP^{RUN-18} to generate mutants bearing M-(E33A, W35A, R38A), M-(I36A) or M-(I36V) mutation by Genecust (Boynes, France). The production of endotoxin-free plasmids, their quantification, and the sequencing were performed by Genecust (Boynes, France). A549 cells were transiently transfected with plasmids using Lipofectamine 3000 (Thermo Fisher Scientific, Les Ulis, France) according to the manufacturer's instructions.

Western blot assay

Cells were seeded in 24-well plates at a density of 1.5×10^5 cells per well, then transfected with vector plasmid constructs. After 18 h of transfection, cell lysates were performed in radioimmunoprecipitation assay (RIPA) lysis buffer (Sigma-Aldrich Humeau, La Chapelle-Sur-Erdre, France) at 4 °C for 10 min. Lysates were centrifuged at 12000 ***g*** for 20 min, at 4 °C. Proteins from total cell extracts were quantified using bicinchoninic acid (BCA) reagent according to manufactured instructions (Sigma-Aldrich Humeau, La Chapelle-Sur-Erdre, France). Protein extracts were treated with Laemmli sample buffer, either under reducing (heated at 95 °C for 5 min, in presence of dithiothreitol [DTT]) or nonreducing conditions (no heat, no DTT). Proteins were separated by in-house 12% SDS-PAGE gel and transferred onto nitrocellulose NC Protan membrane with 0.45 µM pores (Amersham, GE, Buc, France). The membranes were blocked for 20 min with 5% non-fat dry milk in PBS-Tween and incubated with anti-4G2, anti-6x(His) or anti-β actin antibodies (dilution 1:2000) for 1 h at room temperature. Anti-mouse or anti-rabbit IgG HRP-conjugated secondary antibodies were used at 1:10 000 dilution. Membranes were incubated with enhanced chemiluminescence (ECL) prime detection reagents (GE, Buc, France) and exposed using Amersham imager 680 (GE, Buc, Healthcare).

Flow cytometry analysis

Cells were seeded in 24-well plates at a density of 1.5×10^5 cells per well, then transfected with vector plasmid constructs. For detection of GFP expression, cells were gently harvested by trypsinization, fixed with 3.7% paraformaldehyde (PFA) in phosphate-buffered saline (PBS) for 10 min and then observed for the green fluorescent protein. For detection of the E protein, cells were permeabilized with 0.15% Triton X-100 in PBS for 5 min, then blocked with 2% bovine serum albumin (BSA) in PBS, and labelled with anti-4G2 or anti-4E11 antibodies (dilution 1:2000) for 1 h at room temperature. For the detection of NS1 protein, permeabilized cells were labelled with anti-6x(His) antibody (dilution 1:2000). Goat anti-mouse Alexa Fluor 488 IgG antibody was used as a secondary antibody (1:2000) for 30 min. For each assay, 10^4 cells were analysed by flow cytometry using a CytoFLEX flow cytometer (Beckman, Coulter, Brea, CA, USA) using CytExpert software (version 2.1.0.92, Beckman Coulter, Villepinte, France).

RT-qPCR assays

Cells were seeded in 24-well plates at a density of 1.5×10^5 cells per well, then transfected with vector plasmid constructs. Quantification of prM and E RNA was performed by RT-qPCR. After 18 h of transfection, total cellular RNA was extracted from cells with RNeasy kit (Qiagen, Hilden, Germany) according to the manufacturer's recommendations. Total cDNA was obtained by reverse transcription using random hexamers pd(N)6 and M-MLV reverse transcriptase (Life Technologies, Carlsbad, CA, USA) at 42 °C for 50 min. cDNA were amplified using 0.2 µM of each primer (prM: forward primer 5′-CAACAGYGATGGCGTTC-3′, reverse primer 5′-TCCARTCCCATTCCCAC-3′; E: forward primer 5′-GTTACACCCCACTCTGGC-3′, reverse primer 5′-GAAGTCCAGGCCAGTCCG-3′), 2X Absolute Blue qPCR SYBR Green Low ROX Master Mix (ThermoFisher, Waltham, MA, USA) on a CFX96 Real-Time PCR Detection System (Bio-Rad, Life Science, Hercules, CA, USA). The CFX96 software (Bio-Rad) was used to evaluate the threshold cycle (Ct) for each well in the exponential phase of amplification. Results were normalized to the housekeeping gene GAPDH in each condition.

Immunofluorescence confocal assay

Cells were seeded in 24-well plates at a density of 1.5×10^5 cells per well, grown as a monolayer on a glass coverslip and were then transfected with vector plasmid constructs. After 18 h of transfection, cells were fixed on coverslip with 3.7% PFA in PBS for 15 min. Cells were permeabilized with 0.15% Triton X-100 in PBS for 15 min, blocked with 2% BSA in PBS, and then labelled with anti-4G2 and anti-calnexin antibodies (dilution 1:1000) for 1 h at room temperature. Donkey anti-mouse Alexa Fluor 488 and donkey anti-rabbit Alexa Fluor 594 were used as secondary antibodies (1:2000) for 30 min, and the nuclei were stained with DAPI. Then 50% glycerol in PBS was used as mounting media. Capture of the fluorescent signal was allowed with a Nikon Eclipse TI2-S-HU (confocal microscopy) coupled to the imaging software NIS-Element AR (Nikon, Champigny-sur-Marne, France). Line scan profiles were produced using ImageJ software.

LDH assay

Cells were seeded in a 96-well culture plate at a density of 2.5×10^4 cells per well. Cytotoxicity was evaluated by quantification of lactate dehydrogenase (LDH) release in culture supernatant of transfected cells using CytoTox96 nonradioactive cytotoxicity assay

(Promega, Charbonnières-les-Bains, France) according to the manufacturer's instructions. The absorbance of converted dye was measured at 490 nm with background subtraction at 690 nm using a microplate reader Tecan (Tecan Trading AG, Männedorf, Switzerland).

MTT assay

Cells were seeded in a 96-well culture plate at a density of 2.5×10^4 cells per well. Cell monolayers were rinsed with PBS and incubated with supplemented DMEM culture growth medium mixed with 5 $mg.mL^{-1}$ MTT (3-[4,5-dimethylthiazol-2-yl]−2,5-diphenyltetrazolium bromide) solution for 1 h at 37 °C. MTT medium was removed, and the formazan crystals were solubilized with dimethyl sulfoxide (DMSO). Absorbance was measured at 570 nm with background subtraction at 690 nm, using a microplate reader Tecan (Tecan Trading AG, Männedorf, Switzerland).

Caspase 3/7 enzymatic activity

Cells were seeded in a 96-well culture plate at a density of 2.5×10^4 cells per well. Caspase 3/7 enzymatic activity in raw cell lysates was measured using a Caspase Glo 3/7 assay kit (Promega) according to the manufacturer's recommendations. Caspase activity was quantified by luminescence using a FLUOstar Omega Microplate Reader (BMG Labtech, Champigny-sur-Marne, France).

Statistical analysis

Our results were statistically analysed using the GraphPad Prism software (version 9, GraphPad software, San Diego, CA, USA). One-way ANOVA tests were performed to compare quantitative data between the different experimental conditions, with Dunnett or Tukey correction for multiple comparisons. Values of $P<0.05$ were considered statistically significant for ANOVA test. The degrees of significance are indicated in the figure, $****P<0.0001$, $***P<0.001$, $**P<0.01$, $*P<0.05$ or *n.s.*: not significant. All values were expressed as mean ± SEM of at least three independent experiments.

RESULTS

Characterization of recombinant RUN-18 E protein co-expressed with prM

As proper folding of DENV-2 E protein involves the chaperone activity of prM [10, 11], recombinant RUN-18 E protein was co-expressed with prM as a polyprotein precursor which is then processed by cellular signal peptidase [14]. A synthetic gene encoding RUN-18 prM and E proteins with optimized codons for expression in human cells was inserted into the vector plasmid pcDNA3. In the resulting plasmid pcDNA3/RUN-18 prME, the sequence coding for prM followed by E was preceded by the authentic RUN-18 prM signal sequence. In our experiments, human epithelial A549 cell line was chosen for its high permissiveness to DENV replication, making it a suitable model for analysing the expression of recombinant prM and E proteins in human cells.

Expression of recombinant RUN-18 E protein was assessed in A549 cells transfected with pcDNA3/RUN-18 prME for 18 h. A plasmid pcDNA3/RUN-18 NS1 encoding recombinant soluble NS1 protein from RUN-18 was used as a plasmid control since protein expression results in a weak effect on cell viability [29]. Expression of recombinant RUN-18 NS1 in A549 cells transfected with pcDNA3/RUN-18 NS1 was verified by FACS analysis and immunoblot assay (Fig.S1, available in the online version of this article). The antigenic reactivity of recombinant E protein was assessed by FACS analysis using anti-DENV E monoclonal antibodies (mAbs) 4G2 and 4E11 that bind to epitopes into DENV-2 EDII and EDIII, respectively (Fig. 1a). Immunoblot assay using mAb 4G2 allowed the detection of recombinant E protein expressed in A549 cells (Fig. 1b). The cytotoxicity of recombinant RUN-18 prM-E heterodimer was evaluated by quantifying lactate dehydrogenase (LDH) or MTT activity in A549 cells transfected with pcDNA3/RUN-18 prME for 18 h (Fig. 1c). Plasmid pcDNA3/RUN-18 NS1 was used as a control. Comparable levels of LDH or MTT activity were found in A549 cells expressing recombinant RUN-18 prM and E proteins or RUN-18 NS1 protein. Thus, pcDNA3/RUN-18 prME plasmid is suitable for the production of a recombinant DENV-2 E protein belonging to southwestern Indian ocean genotype II.

Effect of M-I36V mutations on RUN-18 E protein co-expressed with prM

To assess the effect of M-I36V mutation (equivalent to prM-I127V mutation), site-directed mutagenesis was performed on plasmid pcDNA3/RUN-18 prME to generate a mutant plasmid bearing a valine at position M36. A plasmid mutant with an alanine at position M36 was used as control. Amino acids 33, 35, and 38 of M protein are highly conserved among flaviviruses, with tryptophan at position M35 being invariable [20]. It has been reported that glutamic acid at position M33 is involved in prM interaction with EDII in the prME heterodimer [30]. Consequently, we generated a pcDNA3/RUN-18 prME mutant bearing the three mutations E33A, W35A, and R38A as a control.

A549 cells were transfected for 18 h with pcDNA3/RUN-18 prM-E or each of the three plasmid mutants. RT-qPCR analysis on total RNA extracted from transfected cells verified that the different plasmids produced similar amounts of mRNA transcripts coding for

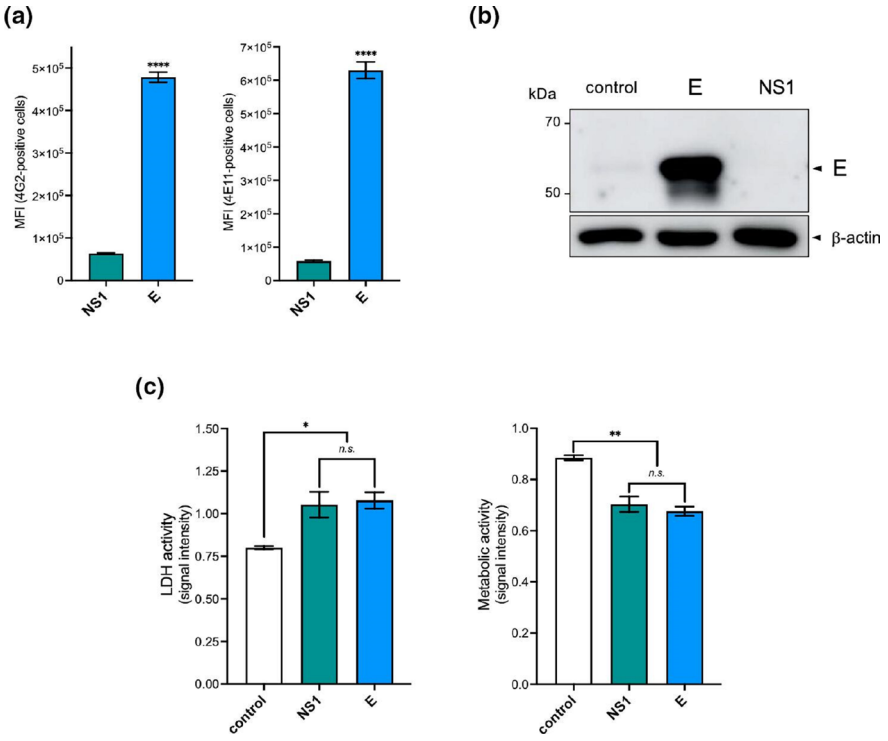

Fig. 1. Expression of recombinant RUN-18 E protein. A549 cells were transfected for 18 h with plasmid pcDNA3/RUN-18 prME expressing recombinant RUN-18 prM and E proteins or mock-transfected (control). A plasmid expressing recombinant DENV-2 RUN-18 NS1 protein served as a control. In (a), intracellular DENV-2 E protein was labelled using anti-E mAbs 4G2 and 4E11. The mean fluorescence intensity (MFI) of FITC signal in cells was examined by FACS analysis. The results are the mean (± SEM) of three independent assays in duplicate. Statistical analysis for E was performed and noted (****P<0.0001). In (b), immunoblot assays on RIPA cell lysates were performed for the detection of the E protein using anti-E mAb 4G2. Data are representative of three independent experiments. β-Actin served as a housekeeping protein. In (c), LDH activity (left) and MTT (right) activity were measured and O.D. values were expressed as signal intensity. The results are the mean (± SEM) of three independent assays with replicates. Statistical analysis for comparing control, E and NS1 was performed and noted (**P<0.01; *P<0.05; *n.s*: not significant).

prM and E proteins (Fig.S2). FACS analysis was first performed on recombinant RUN-18 E protein co-expressed with prM in A549 cells using anti-E mAbs 4G2 and 4E11 (Fig. 2). There was a weak recognition of RUN-18 E protein co-expressed with prM bearing the M-(E33A, W35A, R38A) mutations compared with wild-type RUN-18 prM and E proteins. This suggests a role for M protein in the expression of RUN-18 E protein co-expressed with prM in A549 cells. As it has been observed with the M-(E33A, W35A, R38A) mutant, M-I36V mutation greatly affected the antigenic reactivity of E protein (Fig. 2). In contrast, the mutation M-I36A has no effect on the recognition of recombinant RUN-18 E protein by mAbs 4G2 and 4E11 (Fig. 2). Thus, the nature of amino acid 36 of M protein (equivalent to prM127 residue) influences the expression of RUN-18 E protein.

We next examined the impact of M residue 36 on the subcellular distribution of RUN-18 E protein. Consequently, confocal immunofluorescence (IF) microscopy using anti-E mAb 4G2 was assessed on A549 cells producing recombinant RUN-18 E protein co-expressed with prM (Fig. 3). As one major function of the endoplasmic reticulum (ER) is to serve as a site for synthesis of secreted and membrane proteins, transit of the E protein through the ER compartment was checked using ER-resident calnexin (CNX) antibody. Analysis of the ER also helps to determine proteins that successfully go through the secretory pathway. Dotted E protein-related foci which do not co-colocalize in the cytoplasm with CNX were detected in A549 cells suggesting a trafficking of RUN-18 E protein through the secretory pathway, with no accumulation in the ER (Fig. 3). The co-expression of E with prM mutant bearing the Ala mutations at positions M33/35/38 resulted in accumulation of E protein in the ER compartment as visualized by colocalization with CNX (Fig. 3). This accumulation is correlated with a strong decrease in dotted E protein-related foci suggesting a retention of the E protein. This ER retention seems to be associated with changes in the ER morphology, highlighted by bigger tubular and sheet-like cisternae structures. Whereas the mutation M-I36A has no obvious effect on the subcellular localization of E protein as compared with WT, the mutation M-I36V was associated with phenotypes similar to those observed with Ala mutations at positions M33/35/38 (Fig. 3). Thus, substitution of M-36I residue by a valine but not alanine may drive important changes in the processing of RUN-18 E protein co-expressed with prM in A549 cells as suggested by changes in the subcellular localization and progression through the secretory pathway.

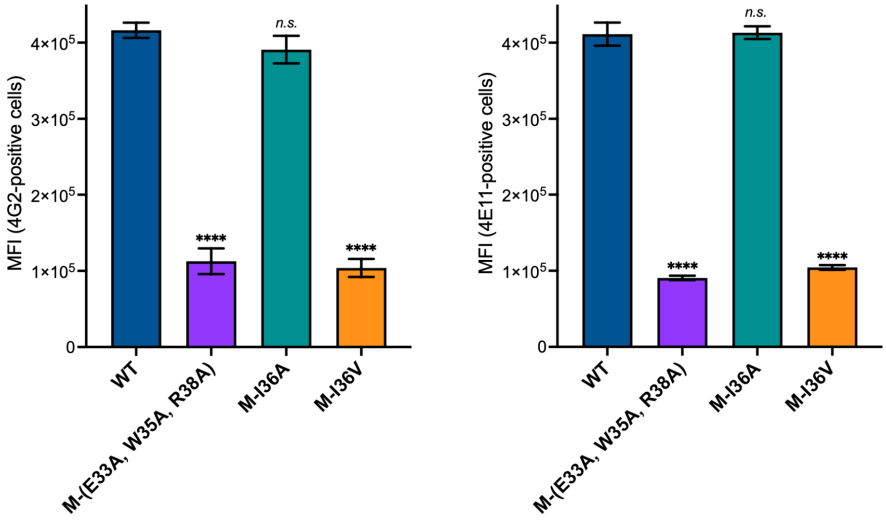

Fig. 2. Effects of ectoM mutations on the expression of recombinant RUN-18 E protein. A549 cells were transfected for 18 h with plasmid pcDNA3/RUN-18 prME expressing recombinant DENV-2 RUN-18 prM and E proteins (WT), plasmid pcDNA3/RUN-18 prME mutants bearing M-I36A, M-I36V, and M-(E33A, W35A, R38A) mutations. FACS analysis was performed on RUN-18 E protein using anti-DENV E mAb 4G2 (left) and 4E11 (right). MFI of intracellular E protein was determined by FACS analysis and the results are the mean (± SEM) of three independent assays in duplicate. Statistical analysis for comparing WT and the mutants was performed and noted (****P<0.0001; *n.s.*: not significant).

Expression of recombinant RUN-18 prM and E proteins was associated with a significant loss of cell viability at 30 h post-transfection (Fig. 4). Measuring LDH and MTT activity, we observed that M-I36V mutation and a lesser extent the M-(E33A, W35A, R38A) mutations but not M-I36A mutation prevented cytotoxic effects induced by prM and E proteins (Fig. 4a). Through the analysis of enzymatic activity of caspases-3/7, we showed that expression of recombinant RUN-18 prM and E proteins can trigger apoptosis in A549 cells at 30 h post-transfection (Fig. 4b). Consistent with the above results, the M-I36V mutation but not M-I36A mutation prevented apoptosis induced by prM and E proteins. Altogether, these results showed that M-I36V mutation alters expression of RUN-18 E protein co-expressed with prM leading to a change in protein subcellular localization associated with an absence of cytopathic effects in A549 cells. The lack of effect of the M-I36A mutation highlights that the nature of amino acid 36 of M protein might have a major impact on the expression and changes in the subcellular distribution of the E protein.

The M residue 36 influences the death-promoting capability of D_2AMP peptide

RUN-18 and DES-14 ectoM sequences differ by a single amino-acid change at position M36 (Fig. 5a). The cluster of amino acids 31 to 41 of RUN-18 M protein (referred hereafter as $D_2AMP^{RUN\text{-}18}$ for Dengue 2 Apoptotic M Peptide of RUN-18) has been identified as a pro-apoptotic peptide (Fig. 5a) [31]. The distribution of D_2AMP in the secretory pathway was a prerequisite for apoptosis induction [16]. To evaluate the impact of valine at position M36 on the death-promoting capability of D_2AMP (Fig. 5a), we dispose of plasmid pcDNA3/sGFP-$D_2AMP^{RUN\text{-}18}$ expressing $D_2AMP^{RUN\text{-}18}$ peptide positioned to the C-terminus of soluble GFP (sGFP) which is preceded by the RUN-18 prM signal peptide [31]. By directed mutagenesis, the M-I36V mutation was introduced into pcDNA3/sGFP-$D_2AMP^{RUN\text{-}18}$ to generate pcDNA3/sGFP-$D_2AMP^{DES\text{-}14}$. As controls, alanine was introduced at positions M33, M35, and M38, or M36 of $D_2AMP^{RUN\text{-}18}$ (Fig. 5a). To estimate the impact of mutations on RUN-18 ectoM conformation, a three-dimensional structure of RUN-18 ectoM was performed by modelling on AlphaFold2 (Fig. 5b) and PDB (Fig. S3) prediction servers. The protein structure predictions suggest that ectoM was unchanged between RUN-18 and DES-14. Also, Ala mutations on positions M33, M35, M36, and M38 would have no effects on amphipathic peri-membrane α-helix of DENV-2 ectoM.

As for the prM-E complexes, sGFP-$D_2AMP^{RUN\text{-}18}$ and sGFP-$D_2AMP^{DES\text{-}14}$ were expressed in A549 cells and then examined for their transit through the ER compartment. The 41 amino acid residues of ectoM fused to the C-terminus of sGFP leading to sGFP-ectoM$^{RUN\text{-}18}$ and sGFP-ectoM$^{DES\text{-}14}$ fusion proteins were used as controls, as well as sGFP lacking $D_2AMP^{RUN\text{-}18}$. Confocal IF microscopy was performed on A549 cells at 18 h post-transfection (Fig. 6). A partial co-localization of sGFP with CNX was observed confirming that soluble reporter protein was correctly processed through the ER compartment. In A549 cells transfected with plasmid expressing sGFP-$D_2AMP^{RUN\text{-}18}$, large dots of GFP-containing structures co-localize with CNX and the ER displays a coarse reticular network at the cell periphery such as crown-like structures (CLS) (Fig. 6). The formation of these CLS might be due to $D_2AMP^{RUN\text{-}18}$-induced aggregations into the ER compartment leading to morphology changes. Expression of ectoM$^{RUN\text{-}18}$ resulted in similar CLS but localization seems a bit different with much less colocalization areas. Only $D_2AMP^{RUN\text{-}18}$ altered the ER organization, with accumulation of a dense structure at the cell periphery (Fig. 6). The substitution of Ala at position M36 of sGFP-$D_2AMP^{RUN\text{-}18}$ resulted in a formation of a

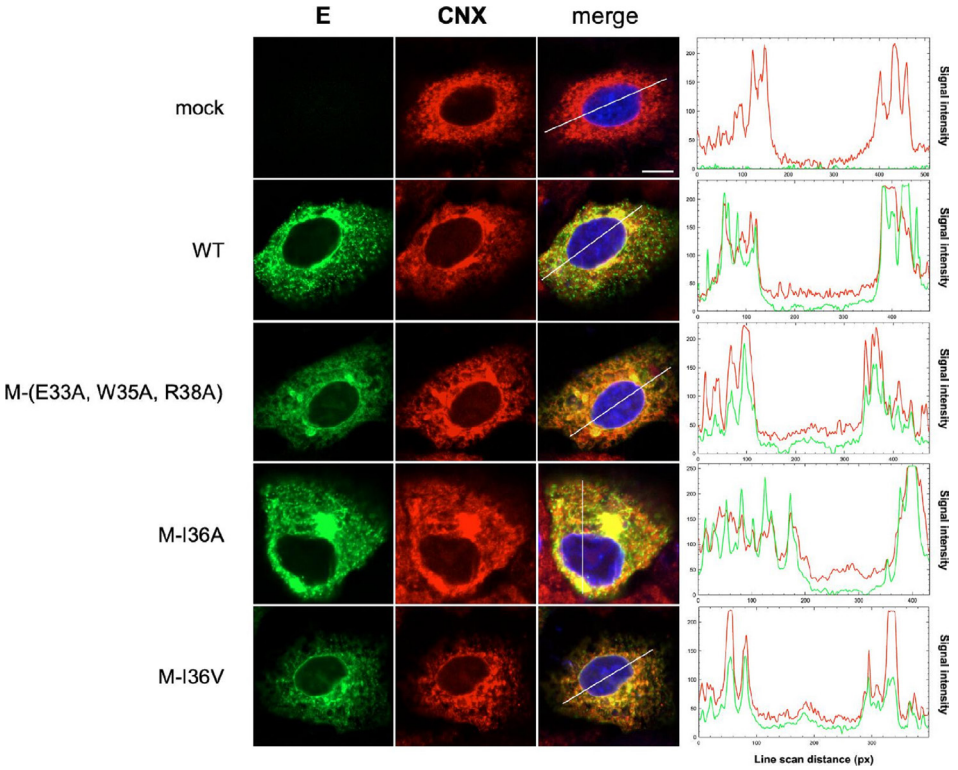

Fig. 3. Effects of ectoM mutations on the subcellular distribution of recombinant RUN-18 E protein. A549 cells were transfected for 18 h with plasmid pcDNA3/RUN-18 prME expressing recombinant DENV-2 RUN-18 prM and E proteins (WT), plasmid pcDNA3/RUN-18 prME mutants bearing M-I36A, M-I36V, and M-(E33A, W35A, R38A) mutations or mock-transfected (mock). For confocal microscopy analysis, cells were fixed, permeabilized and then immunolabelled using anti-E mAb 4G2 and anti-calnexin (CNX) antibody. Cells were visualized for E (green) and CNX (red), and analysed for line-scan profiles of fluorescence intensity. Merged pictures are shown in the right panels with a white line illustrating the location of the line-scan profiles. Scale bar, 5 µm. Data are representative of three independent experiments.

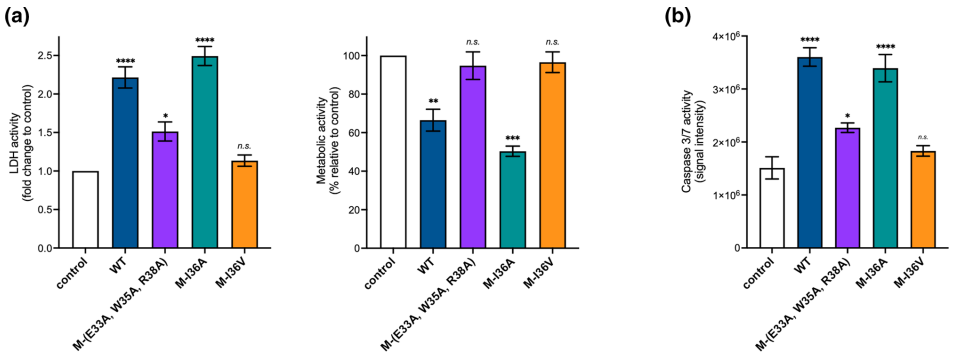

Fig. 4. Effects of ectoM mutations on cytotoxicity of recombinant RUN-18 E protein. A549 cells were transfected for 30 h with plasmid pcDNA3/RUN-18 prME expressing recombinant DENV-2 RUN-18 prM and E proteins (WT), plasmid pcDNA3/RUN-18 prME mutants bearing M-I36A, M-I36V, and M-(E33A, W35A, R38A) mutations or mock-transfected (control). In (a), LDH activity was measured and cell membrane permeability was expressed as a fold change relative to control. The level of cell metabolic activity was measured using MTT assay and expressed as a percentage relative to control. The results are the mean (± SEM) of three independent assays in four replicates. Statistical analysis for comparing control with WT and the three M mutants was performed and noted (****P<0.0001, ***P<0.001, **P<0.01, *P<0.05; *n.s.*: not significant). In (b), caspase-3/7 enzymatic activity was measured and O.D. values were expressed as signal intensity. The results are the mean (± SEM) of three independent assays in four replicates. Statistical analysis for comparing control with WT and the three M mutants was performed and noted (****P<0.0001; *P<0.05; *n.s.*: not significant).

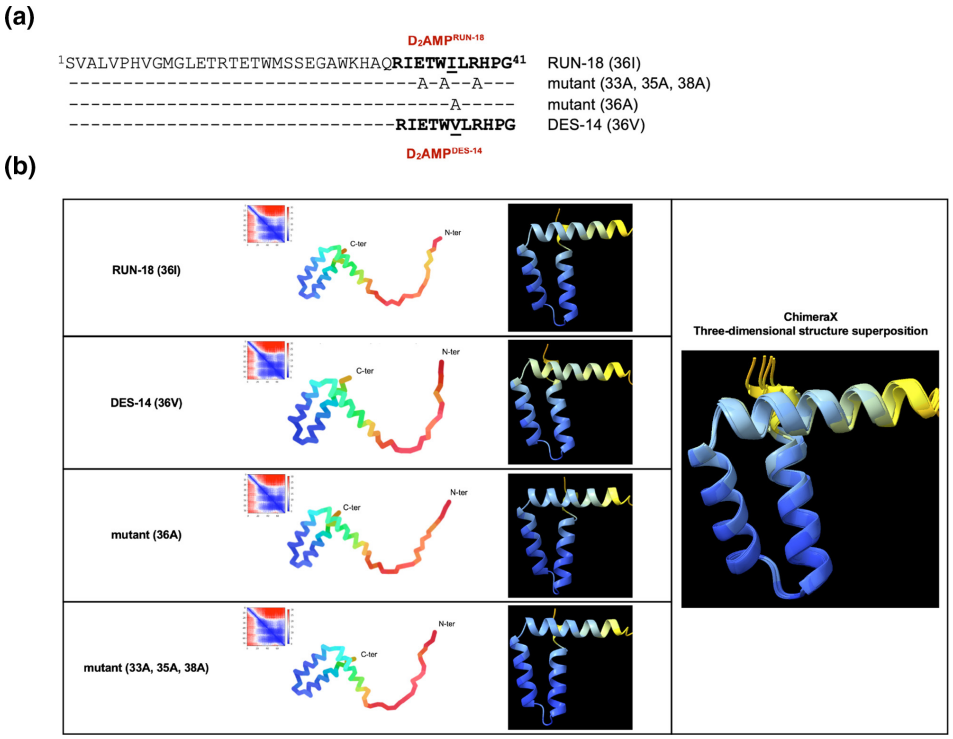

Fig. 5. Impact of ectoM mutations on DENV-2 M structure. In (a), the alignment of ectoM^{RUN-18} and ectoM^{DES-14} sequences and ectoM mutants bearing the mutations at positions M-33, M-35, M-36 and M-38. The D_2AMP peptide sequences are indicated in bold. In (b), 3D structures prediction of RUN-18 M protein, DES-14 M protein, and mutants were obtained from protein database bank (GenBank reference number MN272404.1) and rendered using AlphaFold2 protein prediction server (https://colab.research.google.com/github/sokrypton/ColabFold/blob/main/AlphaFold2.ipynb). In left, the M proteins are depicted as follows: the N-terminal region is red, the α-helix is green and the two TMDs are blue. Predicted aligned error are indicated. In right, protein structures of the four ectoM constructs were aligned and overlapped using ChimeraX software. All pictures were drawn using ChimeraX software.

thinner structure around the nucleus without marked alterations of ER morphology (Fig. 6). These phenotypes were also observed with sGFP-ectoM^{RUN-18} mutant bearing an alanine at position M36 (Fig. 6). Finally, expression of sGFP-D_2AMP^{DES-14} and sGFP-ectoM^{DES-14} gave similar results as those observed with mutant Ala at position M36, sGFP-D_2AMP^{DES-14} giving leading to a more pronounced transit through the secretory pathway as visualized with the high number of green dots (Fig. 6). Thus, D_2AMP^{DES-14} would have a greater propensity to migrate through the secretory pathway as compared with D_2AMP^{RUN-18}.

We assessed whether D_2AMP^{DES-14} and D_2AMP^{RUN-18} can differ by their capacity to trigger apoptosis. Consequently, A549 cells were transfected with plasmids expressing sGFP conjugated with D_2AMP^{DES-14} and D_2AMP^{RUN-18} (Fig. 7). D_2AMP^{RUN-18} mutants bearing alanine on positions M36 and M33/35/38 served as controls (Fig. 5a). Caspase-3/7 activity was detected in A549 cells expressing sGFP-D_2AMP^{RUN-18} (Fig. 7a), associated with a moderate loss of cell viability (Fig. 7b). The presence of alanine at positions M33/35/38 greatly affected the death-promoting capability of D_2AMP^{RUN-18} (Fig. 7). This is consistent with the role of M33/35/38 residues on apoptosis-inducing activity of ZAMP, the ZIKV peptide counterpart of D_2AMP [31]. We observed that sGFP-D_2AMP^{DES-14} exhibited a greater propensity to trigger apoptosis in A549 cells compared with D_2AMP^{RUN-18} (Fig. 7a). Expression of sGFP-D_2AMP^{DES-14} resulted in a decrease in cell metabolic activity reaching upto 40% at 30 h post-transfection (Fig. 7b). The results highlight the influence of M residue 36 on the death-promoting capability of D_2AMP. Apoptosis-inducing activity of D_2AMP may depend on the nature of amino acid 36 of the M protein which seems to be important for the transit of the protein through the secretory pathway.

CONCLUSION

The amino acid 36 of M protein has been proposed to play a major role in the flavivirus replication cycle in mammalian cells [18, 19, 32]. The M residue 36 was essentially identified as an uncharged amino acid with isoleucine (DENV-2, DENV-4, JEV, and WNV), alanine (DENV-1 and DENV-3), leucine (YFV) or valine (TBEV) [20], emphasizing that aliphatic hydrophobic properties of amino-acid residue in position 36 were essential for flavivirus M protein. Comparative analysis of DENV-2 M ectoM sequences highlights that position M36 was much less conserved than other ones (Table S1). With an observed amino acid frequency close to 77%, Ile is the

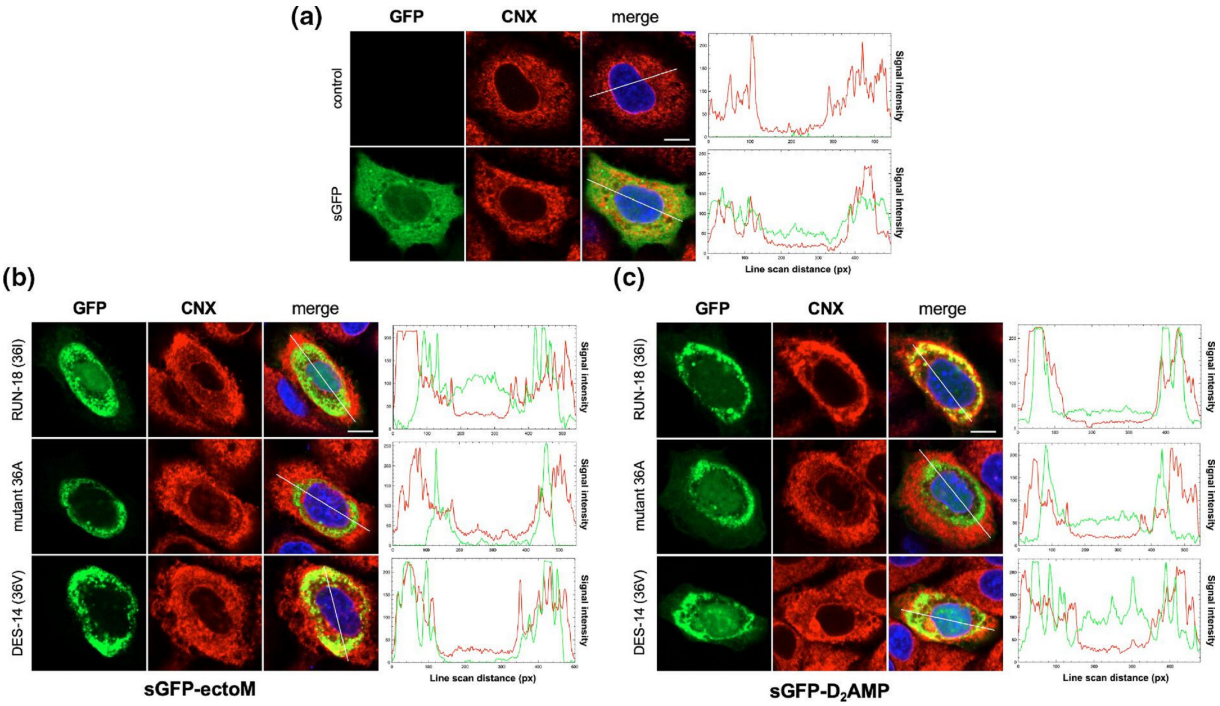

Fig. 6. Subcellular distribution of sGFP-D_2AMP and sGFP-ectoM. A549 cells were transfected for 18 h with plasmids expressing sGFP, sGFP-D_2AMP, or sGFP-ectoM or mock-transfected (mock). The sGFP-D_2AMP and sGFP-ectoM constructs include Ile, Ala, or Val at position M36. For confocal microscopy analysis, cells were fixed, permeabilized and then immunolabeled using anti-CNX antibody. Cells were visualized for E (green) and CNX (red), and analysed for line-scan profiles of fluorescence intensity. Merged pictures are shown in the right panels with a white line illustrating the location of the line-scan profiles. Scale bar, 5 µm. Data are representative of three independent experiments.

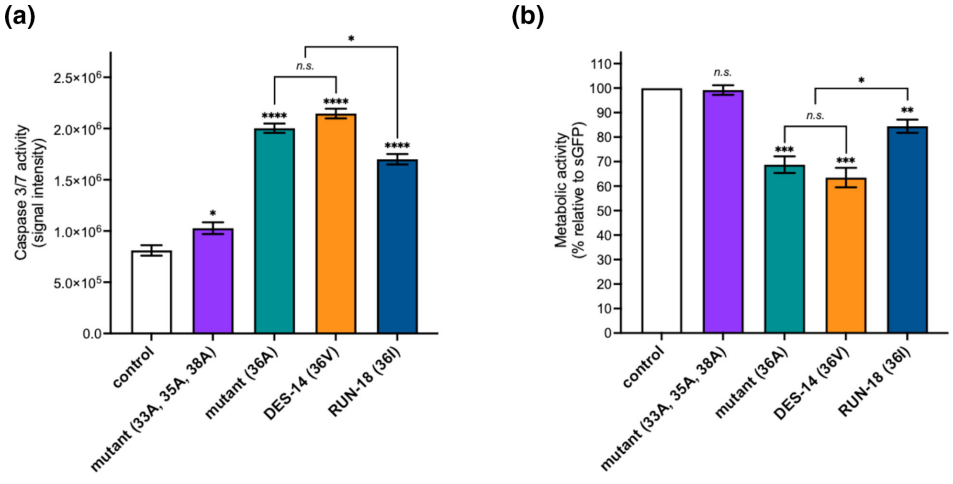

Fig. 7. Impact of M mutations on the cytotoxicity of D_2AMP. A549 cells were transfected for 30 h with plasmids expressing sGFP (control) or sGFP-$D_2AMP^{RUN\text{-}18}$ (RUN-18 (36I)), sGFP-$D_2AMP^{DES\text{-}14}$ (DES-14 (36V)) or sGFP-D_2AMP bearing Ala at positions M33/35/38 (mutant (33A, 35A, 38A)) or M36 (mutant (36A)). In (a), caspase-3/7 enzymatic activity was measured and O.D. values were expressed as signal intensity. The results are the mean (± SEM) of three independent assays in four replicates. Statistical analysis for comparing control with sGFP-D_2AMP was performed and noted (****P<0.0001; *P<0.05; *n.s.*: not significant). In (b), MTT assay was measured and expressed as a percentage relative to control. The results are the mean (± SEM) of three independent assays in four replicates. Statistical analysis for comparing control with-sGFP-D_2AMP was performed and noted (***P<0.001; **P<0.01, *P<0.05; *n.s.*: not significant).

most frequent residue identified at position M36 whereas Val accounted only for 22%. In view of RUN-18 ectoM having Ile at position M36, we wondered whether amino-change Ile-to-Val might have an effect on the biological properties of E co-expressed with prM and the death-promoting capability of D_2AMP.

Analysis of recombinant RUN-18 E protein co-expressed with prM in A549 cells revealed that Ile-to-Val mutation but not Ile-to-Ala mutation at position M36 affected expression and subcellular distribution of E protein suggesting a possible defect in heterodimeric interactions between prM and E proteins. The E proteins of DENV-2 stains RUN-18 and DES-14 differ by four amino-acid substitutions with a particular emphasis towards Gln-to-His change at position E52 in the EDI/EDII interface and Ala-to-Thr change at position E262 in EDII domain which faces the M ectodomain in the prM/E heterodimer (Table S2). It has been proposed that the pr peptide from prM covers the EDII fusion loop preventing E fusion with host cell membranes during the transport of prME heterodimers in the secretory pathway [10]. This suggests a potential role for DES-14 EDII residues E-52H and E-262T as compensatory amino acids to the presence of valine at position M36 in the prME heterodimer of DES-14. Another important finding of the study was the loss of cytotoxicity observed for RUN-18 prM and E proteins with M protein bearing valine at position M36. Such a result was unexpected knowing that a severe defect in flavivirus envelope protein expression usually gives rise to ER stress-induced cellular dysfunction resulting in cell death [33–35]. An explanation is that M-I36V mutation prevents heterodimeric interactions between RUN-18 prM and E proteins leading to rapid protein degradation without prolonged severe ER stress.

D_2AMP is a pro-apoptotic M peptide composed of amino acid residues 31–41 of DENV-2 M ectodomain [16, 17]. Both $D_2AMP^{RUN\text{-}18}$ and $D_2AMP^{DES\text{-}14}$ which only differ by the hydrophobic nature of M residue 36 can trigger apoptosis in A549 cells. However, the presence of valine at position M36 potentiates the apoptosis-inducing activity of $D_2AMP^{DES\text{-}14}$ compared with $D_2AMP^{RUN\text{-}18}$. Using GFP as a reporter protein, different patterns of subcellular distribution of sGFP-D_2AMP have been observed in A549 cells according to the nature of M residue 36. Expression of $D_2AMP^{RUN\text{-}18}$ resulted in large dots that colocalize with ER, highlighting the ER retention. These structures could be a consequence of D_2AMP interactions with cytoskeletal motor protein dynein, which has been described as playing a role in the trafficking of immature viral particles through its interaction with DENV-2 M protein [36–38]. Expression of $D_2AMP^{DES\text{-}14}$ seems to be associated with a better trafficking through the secretory pathway. Our data highlight an important role for M residue 36 in the death-promoting capability of D_2AMP presumably due to protein-protein interactions capable of activating the mitochondrial apoptosis pathway, although exact mechanisms remain to be elucidated [33, 35]. Furthermore, our data do not suggest that D_2AMP-induced apoptosis is related to ER retention but rather that a positive correlation exists between D_2AMP trafficking through the secretory pathway and apoptosis induction. This would be consistent with the notion that distribution of D_2AMP in a post-Golgi compartment is a pre-requisite for inducing apoptosis pathway presumably through interactions with pro-apoptotic factors that are not yet identified [16, 17].

It is now well established that surface structural M protein can contribute to several aspects of the flavivirus replication cycle [18, 19, 39–41]. Our study raises the notion that the hydrophobic nature of M residue 36 may drive expression of DENV-2 E protein and pro-apoptotic activity of D_2AMP. The flavivirus reverse technologies based on ISA method will be useful to generate infectious DENV-2 molecular clones derived from viral strains RUN-18 and DES-14 [42]. Such molecular clones would be reliable tools for further investigation of viral determinants that contribute to the pathogenicity of DENV-2 strains belonging to genotype II (Cosmopolitan) that presently contribute to the global dengue burden. We believe that infectious clones derived from RUN-18 and DES-14 strains will provide important information on the impact of amino acid 36 on the biological properties of DENV-2.

Funding information
This work was supported by the European Regional Development Fund (ERDF) through the RUNDENG project (no. 20202640–0022937) and the POE FEDER 2014–20 of the Conseil Regional de La Réunion (PHYTODENGUE programme, N° SYNERGIE: RE0028005). J.D. was supported by a PhD degree scholarship from La Reunion University (Ecole doctorale STS), funded by the French Ministry MESRI.

Acknowledgements
We thank P. Mavingui and C. El-Kalamouni for their interest in the study. We thank the members of MOCA team for helpful discussions.

Author contributions
J.D., G.G. and P.D. conceived and designed the experiments; J.D. performed the experiments; J.D., G.G. and P.D. analysed the data; P.D. contributed to reagents/materials/analysis tools; J.D., G.G. and P.D. wrote the paper. All authors have read and agreed to the published version of the manuscript.

Conflicts of interest
The authors declare no conflicts of interest.

References

1. Bhatt S, Gething PW, Brady OJ, Messina JP, Farlow AW, *et al*. The global distribution and burden of dengue. *Nature* 2013;496:504–507.
2. Messina JP, Brady OJ, Golding N, Kraemer MUG, Wint GRW, *et al*. The current and future global distribution and population at risk of dengue. *Nat Microbiol* 2019;4:1508–1515.
3. WHO. Dengue and Severe Dengue; 2022. https://www.who.int/news-room/fact-sheets/detail/dengue-and-severe-dengue
4. Chawla P, Yadav A, Chawla V. Clinical implications and treatment of dengue. *Asian Pac J Trop Med* 2014;7:169–178.
5. Rodenhuis-Zybert IA, Wilschut J, Smit JM. Dengue virus life cycle: viral and host factors modulating infectivity. *Cell Mol Life Sci* 2010;67:2773–2786.

6. Pierson TC, Kielian M. Flaviviruses: braking the entering. *Curr Opin Virol* 2013;3:3–12.
7. Allison SL, Schalich J, Stiasny K, Mandl CW, Heinz FX. Mutational evidence for an internal fusion peptide in flavivirus envelope protein E. *J Virol* 2001;75:4268–4275.
8. Mukhopadhyay S, Kuhn RJ, Rossmann MG. A structural perspective of the flavivirus life cycle. *Nat Rev Microbiol* 2005;3:13–22.
9. Murray JM, Aaskov JG, Wright PJ. Processing of the dengue virus type 2 proteins prM and C-prM. *J Gen Virol* 1993;74 (Pt 2):175–182.
10. Li L, Lok S-M, Yu I-M, Zhang Y, Kuhn RJ, *et al*. The flavivirus precursor membrane-envelope protein complex: structure and maturation. *Science* 2008;319:1830–1834.
11. Zhang W, Chipman PR, Corver J, Johnson PR, Zhang Y, *et al*. Visualization of membrane protein domains by cryo-electron microscopy of dengue virus. *Nat Struct Mol Biol* 2003;10:907–912.
12. Konishi E, Mason PW. Proper maturation of the Japanese encephalitis virus envelope glycoprotein requires cosynthesis with the premembrane protein. *J Virol* 1993;67:1672–1675.
13. Lorenz IC, Allison SL, Heinz FX, Helenius A. Folding and dimerization of tick-borne encephalitis virus envelope proteins prM and E in the endoplasmic reticulum. *J Virol* 2002;76:5480–5491.
14. Stadler K, Allison SL, Schalich J, Heinz FX. Proteolytic activation of tick-borne encephalitis virus by furin. *J Virol* 1997;71:8475–8481.
15. Zhang X, Ge P, Yu X, Brannan JM, Bi G, *et al*. Cryo-EM structure of the mature dengue virus at 3.5-Å resolution. *Nat Struct Mol Biol* 2013;20:105–110.
16. Catteau A, Kalinina O, Wagner M-C, Deubel V, Courageot M-P, *et al*. Dengue virus M protein contains a proapoptotic sequence referred to as ApoptoM. *J Gen Virol* 2003;84:2781–2793.
17. Catteau A, Roué G, Yuste VJ, Susin SA, Desprès P. Expression of dengue ApoptoM sequence results in disruption of mitochondrial potential and caspase activation. *Biochimie* 2003;85:789–793.
18. de Wispelaere M, Khou C, Frenkiel M-P, Desprès P, Pardigon N, *et al*. A single amino acid substitution in the M protein attenuates Japanese encephalitis virus in mammalian hosts. *J Virol* 2016;90:2676–2689.
19. Basset J, Burlaud-Gaillard J, Feher M, Roingeard P, Rey FA, *et al*. A molecular determinant of West Nile virus secretion and morphology as a target for viral attenuation. *J Virol* 2020;94:e00086-20.
20. Hsieh S-C, Zou G, Tsai W-Y, Qing M, Chang G-J, *et al*. The C-terminal helical domain of dengue virus precursor membrane protein is involved in virus assembly and entry. *Virology* 2011;410:170–180.
21. Yenamandra SP, Koo C, Chiang S, Lim HSJ, Yeo ZY, *et al*. Evolution, heterogeneity and global dispersal of cosmopolitan genotype of Dengue virus type 2. *Sci Rep* 2021;11:13496.
22. Giovanetti M, Pereira LA, Santiago GA, Fonseca V, Mendoza MPG, *et al*. Emergence of dengue virus serotype 2 cosmopolitan genotype, Brazil. *Emerg Infect Dis* 2022;28:1725–1727.
23. Pascalis H, Turpin J, Roche M, Krejbich P, Gadea G, *et al*. The epidemic of Dengue virus type-2 cosmopolitan genotype on Reunion Island relates to its active circulation in the Southwestern Indian Ocean neighboring islands. *Heliyon* 2019;5:e01455.
24. Pascalis H, Biscornet L, Toty C, Hafsia S, Roche M, *et al*. Complete genome sequences of Dengue virus type 2 epidemic strains from Reunion Island and the seychelles. *Microbiol Resour Announc* 2020;9:e01443-19.
25. Vairo F, Mboera LEG, De Nardo P, Oriyo NM, Meschi S, *et al*. Clinical, virologic, and epidemiologic characteristics of Dengue outbreak, Dar es Salaam, Tanzania, 2014. *Emerg Infect Dis* 2016;22:895–899.
26. Santé Publique France. Surveillance de la dengue à La Réunion; 2023. https://www.santepubliquefrance.fr/recherche/#search=Dengue%20%C3%A0%20La%20R%C3%A9union&themes=dengue®ions=Oc%C3%A9an%20Indien
27. Hafsia S, Haramboure M, Wilkinson DA, Baldet T, Yemadje-Menudier L, *et al*. Overview of dengue outbreaks in the southwestern Indian Ocean and analysis of factors involved in the shift toward endemicity in Reunion Island: a systematic review. *PLoS Negl Trop Dis* 2022;16:e0010547.
28. ARS. Situation de La Dengue à La Réunion; 2019. https://www.lareunion.ars.sante.fr/point-sur-la-dengue-la-reunion-1
29. Ogire E, Diaz O, Vidalain P-O, Lotteau V, Desprès P, *et al*. Instability of the NS1 glycoprotein from La Reunion 2018 Dengue 2 virus (Cosmopolitan-1 Genotype) in huh7 cells is due to lysine residues on positions 272 and 324. *Int J Mol Sci* 2021;22:1951.
30. Peng J-G, Wu S-C. Glutamic acid at residue 125 of the prM helix domain interacts with positively charged amino acids in E protein domain II for Japanese encephalitis virus-like-particle production. *J Virol* 2014;88:8386–8396.
31. Vanwalscappel B, Haddad JG, Almokdad R, Decotter J, Gadea G, *et al*. Zika M oligopeptide ZAMP confers cell death-promoting capability to a soluble tumor-associated antigen through caspase-3/7 activation. *Int J Mol Sci* 2020;21:9578.
32. Hsieh S-C, Wu Y-C, Zou G, Nerurkar VR, Shi P-Y, *et al*. Highly conserved residues in the helical domain of dengue virus type 1 precursor membrane protein are involved in assembly, precursor membrane (prM) protein cleavage, and entry. *J Biol Chem* 2014;289:33149–33160.
33. Okamoto T, Suzuki T, Kusakabe S, Tokunaga M, Hirano J, *et al*. Regulation of apoptosis during flavivirus infection. *Viruses* 2017;9:243.
34. Turpin J, El Safadi D, Lebeau G, Krejbich M, Chatelain C, *et al*. Apoptosis during ZIKA virus infection: too soon or too late? *Int J Mol Sci* 2022;23:1287.
35. Pan Y, Cheng A, Wang M, Yin Z, Jia R. The dual regulation of apoptosis by flavivirus. *Front Microbiol* 2021;12:654494.
36. Johnston JA, Illing ME, Kopito RR. Cytoplasmic dynein/dynactin mediates the assembly of aggresomes. *Cell Motil Cytoskeleton* 2002;53:26–38.
37. Egan MJ, McClintock MA, Hollyer IHL, Elliott HL, Reck-Peterson SL. Cytoplasmic dynein is required for the spatial organization of protein aggregates in filamentous fungi. *Cell Rep* 2015;11:201–209.
38. Ripon MKH, Lee H, Dash R, Choi HJ, Oktaviani DF, *et al*. N-acetyl-D-glucosamine kinase binds dynein light chain roadblock 1 and promotes protein aggregate clearance. *Cell Death Dis* 2020;11:619.
39. Pan P, Zhang Q, Liu W, Wang W, Lao Z, *et al*. Dengue virus M protein promotes NLRP3 inflammasome activation to induce vascular leakage in mice. *J Virol* 2019;93:e00996-19.
40. Brown E, Beaumont H, Lefteri D, Bentham M, Foster R, *et al*. Flavivirus membrane (M) proteins as potential ion channel antiviral targets. *Access Microbiol* 2019;1.
41. Zheng A, Yuan F, Kleinfelter LM, Kielian M. A toggle switch controls the low pH-triggered rearrangement and maturation of the dengue virus envelope proteins. *Nat Commun* 2014;5:3877.
42. Aubry F, Nougairède A, de Fabritus L, Querat G, Gould EA, *et al*. Single-stranded positive-sense RNA viruses generated in days using infectious subgenomic amplicons. *J Gen Virol* 2014;95:2462–2467.